Toy-planet: A Numerical Study of Density Stratification using Smooth Particle Hydrodynamics

Vashisth Tiwari
Classical Dynamics(Physcis 235), University of Rochester (Rochester, NY)

(Dated: March 16, 2023)

In this paper we study the question of density based stratification of planetary cores using Smooth particle hydrodynamics, a grid free Lagrangian method. This study is done with the assumptions of adiabatic pressure, the simplest N-body interaction, no viscosity and electromagnetic interactions. The basics of SPH (kernel functions and particle approximation) are also discussed along with the derivation of the equations of motion in the toy planet model considered. Moreover, we do a numerical study of the stratification and the various factors that might affect it including the density and adiabatic factor. Lastly, the advantages and shortcomings of the toy-planet model and the method of Smooth particle hydrodynamics is discussed along with some suggestions for future improvement.

Keywords: Classical Mechanics, Smooth Particle Hydrodynamics, Planet Formation, Numerical Simulation

I. INTRODUCTION

"Why is the earth's core more dense than the crust?" The physics of stratification of planetary cores, for example the earth's dense core, is still disputed and we are not so sure about the answer to the above question. The study of how planets and stars evolve is of key interest to astrophysics, geophysics and is an ongoing area of inquiry. The question of formation, stratification of planetary cores is a complex problem which depends on various parameters like the pressure, temperature, magnetic strength, etc. Various numerical techniques are employed to study these settings and to better calibrate our scientific understanding of this phenomena. In this paper, we study a small part of this complex system. Even without the added complexity of temperature, electro-magnetic charges, the evolution of particles of different densities is a non trivial problem. We study how a random arrangement of different mono atomic particles evolves under an adiabatic pressure and seeing how order emerges from a random distribution of particles.

The formulation of how the velocity, temperature, pressure, and density of a moving fluid are related is given by the Navier-Stokes Equations [1]:

$$\rho\frac{d\vec{v}}{dt} = -\vec{\nabla}P + \vec{f}_{external} + \mu\nabla^2 \cdot v_i \tag{I.1}$$

Here $\vec{v}$ is the particle velocity, P is the pressure, $\vec{f}$ is force density. These equations were derived independently by G.G. Stokes, in England, and M. Navier, in France, in the early 1800's [1].

To numerically study these family of problems, two computational approaches have evolved: Eulerian methods, Lagrangian methods. Eulerian methods employ grids where fluid parameters are evaluated over grids. Lagrangian methods on the other hand evolve in a moving frame and dispense with fixed points in space [2]. Smooth particle hydrodynamics (SPH), a Lagrangian method, was invented to simulate non-axis-symmetric phenomena in astrophysics by Lucy, Gingold, and Monaghan, specifically to study the dynamical fission instabilities in fast rotating stars [3], [4]. The key idea of SPH is to calculate pressure gradient forces by kernel estimation, directly from the particle positions. This is in stark contrast to finite differentiation on the grid. SPH has has become a widely used tool as it allows the incorporation of various different physical constraints and concepts, does not need the grid to calculate derivatives as it uses analytical differentiation of interpolation functions. SPH has become a standard tool in astronomy, astrophysics and is used in wide areas of research including stellar formation and interaction, planetary formations, supernova explosions, galaxy formation, etc [5].

This paper studies the evolution of particle interaction in a planet like setting using Smooth particle hydrodynamics. Section II introduces the assumptions made in our toy-planet model, encapsulates the overview of the SPH method. We then derive the equations of motion (SPH approximation of the equations from (I.1)) that govern the particles under our assumptions made in the toy-planet and SPH. Section III discusses the implementation and results of the SPH based simulation. Lastly, section IV sheds light on how the results of our simple model compare against what we expect from the given physics and observations, and discusses the limitations of the model and the method used for numerical analysis.

II. BACKGROUND: ASSUMPTIONS AND THE THEORY OF SMOOTH PARTICLE HYDRODYNAMICS

A. Assumptions

In order to understand this complex system, we use the simplified model where the compressibility of the body is not considered but the attractive potential is retained. This system has been of interest to various researchers in the part from Reimann to Dirichlet [6]. In order to understand the state evolution of the particles, we study the simplest many-body force which was discovered by Newton in his monumental work (Principia) in [7]. The fluid equivalent of this potential energy of $j_t h$ particle of the corresponding interaction of an N body system is $U = \frac{G}{2} m_j \sum_j \rho_i ||\vec{x_i} - \vec{x_j}||^2$. Here G is the gravitation constant, where ρ_i (x_i) where are densities (positions) of particle I; m_j (x_j) are masses (positions) of particle j [6].

This model also assumes the flow to be isotropic in the absence of shocks and thermal conduction for this particular analysis; then the pressure, P, which relates mass density ρ and temperature via state equation is given below where K, γ are constants:

$$P = K\rho^{\gamma} \tag{II.1}$$

The formulation of the motion for in-compressible fluid flow over time t is governed by (I.1).

Here we consider an inviscid fluid setting (thus $\mu = 0$), the $\mu\nabla^2 \cdot v_i$ terms go to 0.

B. Smooth Particle Hydrodynamics (SHP)

The key to SPH lies in the mapping of continuum of particles to a discrete series of particles. This discretization is needed as we cannot really deal with a continuum in numerically. The interpolation is based on the theory of using kernels that approximate a delta function, which is then converted to finite summation (discussed in section II B 2). In this section we discuss some key concepts related to SPH: kernel functions and the properties they need to satisfy, particle approximation, and lastly we derive some equations to describe the trajectory of particles in our given settings.

1. Kernel Functions

A generic function $f(\vec{x})$ of position $\vec{x}$ used in the SPH method follows the identity [8]:

$$f(\vec{x}) = \int_\Omega \delta(\vec{x} - \vec{x'}) f(\vec{x'})\, d\Omega_{x'} \tag{II.2}$$

Here f is defined on the n-dimensional domain Ω, and $d\Omega_{x'}$ is the small volume element around x'. This δ function behavior is approximated by the radial basis functions [8] (which are smooth) is the kernel W for $\vec{r} = \vec{x} - \vec{x'}$, $r = ||\vec{r}||$, smoothing length h:

$$\langle f(x) \rangle = \int_\Omega W(r, h) f(\vec{x'})\, d\Omega_{x'} \tag{II.3}$$

These kernel functions functions have to satisfy certain important conditions to be a good candidate for SPH: [1]

1. Delta Function Property: It is apparent that since these functions are used for approximation delta functions, they need to approximate δ function to a good degree. Figure 1 highlights the need for this property. In the mathematical formulation, this requirement is given as [10]:
$$\lim_{h \to 0} W(\vec{r}, h) = \delta(r) \tag{II.4}$$

2. Normalization Condition: Since SPH is a probabilistic approach, another condition that the kernel function has to suffice is [2]
$$\int_\Omega W(r, h)\, d\Omega_{x'} = 1 \tag{II.5}$$

For the sake of making these functions easier to scale by a factor, say α, we write the function $W_{\alpha,r} = W(r, \alpha)$. Some commonly used radial basis functions are as follows [11]

[1] Note: There are other properties that are desirable in kernel functions but are either beyond the scope of this paper or are not relevant to the discussion. For more details, refer to [9]

(Note: $\Phi_{\alpha,x_0}(x) = \phi(||x - x_0||_d/\alpha)$; we define $\Phi_{\alpha,r} = \phi(r/\alpha)$)

i. Gaussian

$$\Phi_{\alpha,r} = e^{\frac{-r^2}{\alpha^2}} \tag{II.6}$$

This was the function that was first used by the authors of SPH.

ii. Inverse Quadratic:

$$\Phi_{\alpha,r} = \frac{1}{\sqrt{1 + \frac{r^2}{\alpha^2}}} \tag{II.7}$$

iii. Wendland Compactly supported functions

$$\Phi_{\alpha,r} = \begin{cases} \left(1 - \frac{r}{\alpha}\right)^4 \left(1 + 4\frac{r}{\alpha}\right) & , r < \alpha \\ 0 & , \text{Otherwise} \end{cases} \tag{II.8}$$

This family of functions is widely used due to their narrower profile (they resemble Gaussian but are narrower), fall off to zero outside the region of interest, along with computationally less expensive derivative calculation.

To be a kernel function, the radial-basis functions have to satisfy the properties discussed above. Thus, we can obtain a kernel function from the radial basis functions by using the following normalization trick (in 3-D setting): [2].

$$W_{\alpha,x} = \frac{\Phi_{\alpha,x}}{\alpha^3 \int_0^\infty 4\pi r^2 \phi(r) dr} \tag{II.9}$$

We also need the gradient of this kernel function in order to approximate the physical properties of the system we are studying. The derivative of the radial basis function has no effect on non-spatially varying constants; thus we get: [11]

$$\vec{\nabla}\Phi_{\alpha,x_j}(x) = (d_r\phi)(||\vec{x} - \vec{x}_j||/\alpha)\vec{\nabla}||\vec{x} - \vec{x}_j||/\alpha \tag{II.10}$$

$$\vec{\nabla}W_{\alpha,x_j} = \frac{1}{\alpha^4 \int_0^{+\infty} 4\pi r^2 \phi(r) dr}(d_r\phi)(||\vec{x} - \vec{x}_j||/\alpha)\frac{\vec{x} - \vec{x}_j}{||\vec{x} - \vec{x}_j||} \tag{II.11}$$

2. Particle Approximation/ Meta- particle

The discrete sum approximation of the kernel approximation that we saw in the II B 1 is done using the "particle approximation". Thus, the approximation of the continuous field given in equation (II.2) is done by discretizing the field by a series of particles is given as:

$$f(\vec{r}) = \sum_i \frac{m_i}{\rho_i} f(\vec{r_i}) W(\vec{r} - \vec{r_i}, h) \tag{II.12}$$

[2] In 2-D, $\alpha^3 \int_0^\infty 4\pi r^2 \phi(r) dr$ in the denominator can be replaced by $\alpha^2 \int_0^\infty 2\pi r \phi(r) dr$ and so on

where $f(\vec{r_i})$, m_i are the function values and the masses of the i^{th} particle. $\rho_i(\vec{r_i})$ is defined as the density and is given as:

$$\rho_i = \sum_j m_j W_{\alpha,x_j}(\vec{x_i}) = \sum_j m_j W_\alpha(\vec{x_i} - \vec{x_j}) \tag{II.13}$$

2, shows a basic schematic of how continuous flows are approximated using these meta particles.

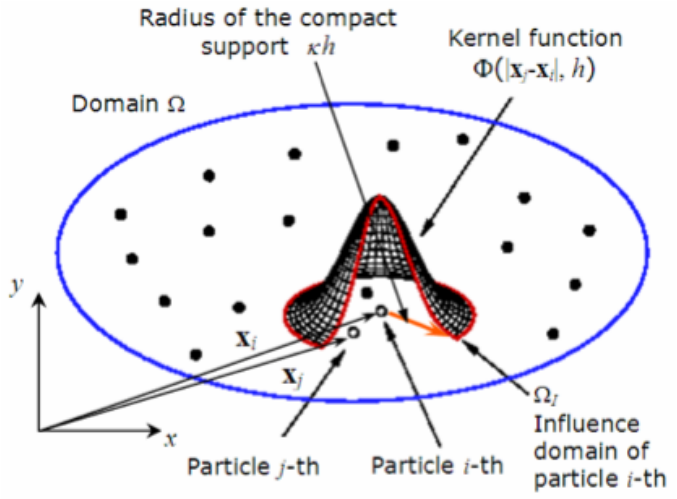

FIG. 1: Demonstrating the kernel function and other relevant details of particle approximation of SPH [8]. Here we have a region of interest that is defined by α in simulation section in III, we see a δ function like behavior as the values quickly fall off as we move from the particle of interest (x_i in this case)

.

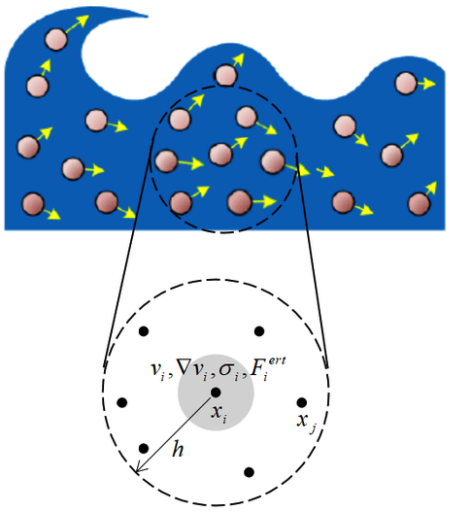

FIG. 2: Schematic showing the discretization of the fluid using SPH [12]

. Here x_i is the reference particle, x_j is the neighbouring particle, v_i is the velocoity, σ_i is viscocity (F_{ext}, h defined before).

3. Equation of motion

The Lagrangian of the system with in-viscid (no viscosity between the particles) is given by the following equation which was derived in 1960 which is given by the difference between the kinetic energy of the particle minus the internal energy (u) [13]:

$$\mathcal{L}(\vec{r}, \vec{v}; t) = \int \frac{1}{2}\rho\vec{v}^2 - \rho u d\vec{r} \tag{II.14}$$

In the SPH approximation, we take $m_i = \rho d\vec{r}$ giving us:

$$\mathcal{L} = \sum_i \left(\frac{1}{2} m_i \vec{v_i}^2 - m_i u_i\right) \tag{II.15}$$

Here, the mass of each particle is given by m_i and we define u_i as the thermal energy per unit pass. The pressure as discucsed in the introduction is given by $P = K\rho^\gamma$ $(II.16)$. This pressure can be rewritten as $P = (\gamma - 1)u\rho$ $(II.17)$ [2].

However, since our system also has the additional potential to gravitation interaction (negative as the Lagrangian is the difference of kinetic and potential energies),

$$\mathcal{L} = \left(\sum_i \left(\frac{1}{2}m_i\vec{v_i}^2 - m_i u_i\right)\right) - \frac{G}{2}m_j \sum_j \rho_i(\vec{x_i} - \vec{x_j})^2 \tag{II.18}$$

The Lagrangian equations of motion for a generalized coordinate q_i are given by the

$$\frac{d}{dt}\frac{\partial L}{\partial \dot{q_i}} - \frac{\partial L}{\partial q_i} = 0 \tag{II.19}$$

For our coordinate for particle j, $\vec{r_j}$ and corresponding velocity $\dot{\vec{r_j}} = \vec{v_j}$. Noting that the second term (with $m_i u_i$, the internal energy) and the third term (the potential term) have no explicit velocity dependence. Additionally, using that the velocities of the particles are independent (i.e., $\frac{\partial v_i}{\partial \vec{v}_{j\neq i}} = 0$)we get that:

$$\begin{aligned}\frac{\partial \mathcal{L}}{\partial \vec{v_j}} &= \frac{\partial}{\partial \vec{v_j}}\left[\sum_i \left(\frac{1}{2}m_i\vec{v_i}^2 - m_i u_i\right)\right] \\ &\quad - \frac{\partial}{\partial \vec{v_j}}\left[\frac{G}{2}m_j \sum_j \rho_i(\vec{x_i} - \vec{x_j})^2\right] \\ &= m_j\vec{v_j}\end{aligned} \tag{II.20}$$

Now onto the second term

$$\begin{aligned}\frac{\partial \mathcal{L}}{\partial \vec{r_j}} &= \frac{\partial}{\partial \vec{r_j}}\left[\sum_i \left(\frac{1}{2}m_i\vec{v_i}^2 - m_i u_i\right) - \frac{G}{2}m_j \sum_j \rho_i(\vec{x_i} - \vec{x_j})^2\right] \\ &= \frac{\partial \mathcal{L}_1}{\partial \vec{r_j}} + \frac{\partial \mathcal{L}_2}{\partial \vec{r_j}}\end{aligned} \tag{II.21}$$

By the extension of notation, we have broken down the terms in $\mathcal{L}_1, \mathcal{L}_2$ for the ease of reference. Now, using the relationship of the pressure term and realizing no explicit r dependence on the first term (the kinetic energy term), we can rewrite the above expression as the following:

$$\frac{\partial \mathcal{L}_1}{\partial \vec{r_j}} = -\frac{\partial}{\partial \vec{r_j}}\left[\sum_i m_i u_i\right] \tag{II.22}$$

$$= -\sum_i m_i \frac{\partial}{\partial \vec{r_j}} u_i \tag{II.23}$$

$$\frac{\partial \mathcal{L}_1}{\partial \vec{r}_j} = -\sum_i m_i \left(\frac{\partial u_i}{\partial P_i} \frac{\partial P_i}{\partial \vec{r}_j} + \frac{\partial u_i}{\partial \rho_i} \frac{\partial \rho_i}{\partial \vec{r}_j} \right) \tag{II.24}$$

$$= -\sum_i m_i \left(\frac{\partial u_i}{\partial P_i} \frac{\partial P_i}{\partial \rho_i} \frac{\partial \rho_i}{\partial \vec{r}_j} + \frac{\partial u_i}{\partial \rho_i} \frac{\partial \rho_i}{\partial \vec{r}_j} \right) \tag{II.25}$$

$$= -\sum_i m_i \left(\frac{\partial u_i}{\partial P_i} \frac{\partial P_i}{\partial \rho_i} + \frac{\partial u_i}{\partial \rho_i} \right) \frac{\partial \rho_i}{\partial \vec{r}_j} \tag{II.26}$$

Now, using the pressure equations (II.16), (II.17)

$$\frac{\partial u_i}{\partial P_i} \frac{\partial P_i}{\partial \rho_i} + \frac{\partial u_i}{\partial \rho_i} = \frac{P_i^2}{\rho_i^2} \tag{II.27}$$

Now lastly, using the relationship from particle approximation (II.13):

$$\frac{\partial \rho_i}{\partial \vec{r}_j} = \sum_k m_k \frac{\partial W_\alpha(\vec{x_k} - \vec{x_i})}{\partial \vec{r}_j} \tag{II.28}$$

Combining the results from (II.26), (II.27), (II.28), we get:

$$\frac{\partial \mathcal{L}_1}{\partial \vec{r}_j} = -\sum_i m_i \left(\frac{P_i^2}{\rho_i^2} \right) \sum_k m_k \frac{\partial W_\alpha(\vec{x_k} - \vec{x_i})}{\partial \vec{r}_j} \tag{II.29}$$

Using the properties of kernel function (i.e., δ function behavior), it was shown that the above expression simplifies to the following [2], [14]:

$$\frac{\partial \mathcal{L}_1}{\partial \vec{r}_j} = -\sum_i m_i \Big(\frac{P_i}{\rho_i^2} + \frac{P_j}{\rho_j^2} \Big) \vec{\nabla} W_\alpha(\vec{x}_i - \vec{x}_j) \tag{II.30}$$

Using the definition of r,

$$\frac{\partial \mathcal{L}_2}{\partial \vec{r}_j} = \frac{G}{2} 2 \sum_i \rho_i m_j (\vec{x}_i - \vec{x}_j) \tag{II.31}$$

$$= G \sum_i \rho_i m_j (\vec{x}_i - \vec{x}_j) \tag{II.32}$$

Now, we can use (II.19), to get the relationship that describes the trajectory of particles:

$$\frac{d}{dt} \frac{\partial \mathcal{L}}{\partial \vec{v}_j} = \frac{\partial \mathcal{L}}{\partial \vec{r}_j} = \frac{\partial \mathcal{L}_1}{\partial \vec{r}_j} + \frac{\partial \mathcal{L}_2}{\partial \vec{r}_j} \tag{II.33}$$

$$m_j \frac{\mathrm{d}\vec{v}_j}{\mathrm{d}t} = -m_j \sum_i m_i \Big(\frac{P_i}{\rho_i^2} + \frac{P_j}{\rho_j^2}\Big) \vec{\nabla} W_\alpha(\vec{x}_i - \vec{x}_j) + m_j G \sum_i \rho_i(\vec{x}_i - \vec{x}_j) \tag{II.34}$$

$$\frac{\mathrm{d}\vec{v}_j}{\mathrm{d}t} = -\sum_i m_i \Big(\frac{P_i}{\rho_i^2} + \frac{P_j}{\rho_j^2}\Big) \vec{\nabla} W_\alpha(\vec{x}_i - \vec{x}_j) + G \sum_i \rho_i(\vec{x}_i - \vec{x}_j) \tag{II.35}$$

The equation above (II.35) describes the trajectory of the particle, and will be at the center of our numerical simulation section that is followed below.

III. SPH SIMULATION

A. Time Step

After tackling the rather tedious math, we can now go to the numerical analysis of the problem at hand. Before diving deeper into how different factors affect the analysis of the problem, we note that the evolution of the factors considered ρ_i, v_i, x_i, etc. are obtained using integration in the analysis. Small time steps not only give better accuracy of time evolution but are also needed as lighter particles "react faster" as compared to heavier ones, which can make the code unstable. The most general criteria for time stepping in gas-dynamical systems is given by Courant-Friedrichs-Lewy or CFL condition (upper bound 1) [2]:

$$c = \frac{\delta_x}{\delta_t} \tag{III.1}$$

In our analysis, we take $dt = 0.1$; we started with a high value of 0.5 and then decreased by decrements of 0.05. We see that the state evolution does not change considerably between $dt = 0.1$ and $dt = 0.05$, so we choose c=0.1 for our analysis. Lower dt is also needed for higher spatial resolution (low δ_x), given we around bounded by the CFL value.

To make sure the code is stable, we define a function (*get_min_dt*) such that $dt_{min} = \frac{1}{100}\frac{\text{length}}{\text{velocity}}$, to make sure that time step is sufficiently small. The time step , dt, is choosen as the minimum of 0.1 and dt_{min}.

B. The Setting of the Simulation

The simulation assumes an adiabatic value $\gamma = 5/3$, which corresponds to an ideal mono atomic gas. The pressure is given by (II.16). A class particle is created which stores all the physical properties associated with the particle like the mass, velocity and positions (in x, y, z), pressure, etc. Due to limited computing power, we assume a rather small sample with $N = 100000$ which are approximated by $N_M = 200$ meta particles. In this simulation, we look at an earth like planet (in terms of the order of magnitude of the total mass of the N particle system is fixed at the mass of the earth, 6×10^{24} kg). The choice of N, N_M was governed by the limitations in computing ability and the time complexity of the algorithm.

Due the reasons discussed in II B 1, we use the Wedland function in 3 dimensions. Using the wedland radial basis function in (II.8), and the normalization condition from (II.9), we

get the kernel function in (III.4) [3].

$$\alpha^3 \int_0^\infty 4\pi r^2 \phi(r) dr = \alpha^3 \left(\int_0^\alpha 4\pi r^2 \phi(r) dr + \int_0^\infty 4\pi r^2 \phi(r) dr \right) \tag{III.2}$$

$$\alpha^3 \int_0^\infty 4\pi r^2 \phi(r) dr = \frac{2\alpha^3 \pi}{21} \tag{III.3}$$

$$\implies W_{\alpha,r} = \begin{cases} \frac{21}{2\pi\alpha^3} \left(1 - \frac{r}{\alpha}\right)^4 \left(1 + 4\frac{r}{\alpha}\right) & , r < \alpha \\ 0 & , \text{Otherwise} \end{cases} \tag{III.4}$$

Using this, we get that:

$$\frac{dW_{\alpha,r}}{dr} = \begin{cases} \frac{210}{\pi\,\alpha^4} \left(\frac{r}{\alpha} - 1\right)^3 \frac{r}{\alpha} & , r < \alpha \\ 0 & , \text{Otherwise} \end{cases} \tag{III.5}$$

At the start of the simulation, we assume spherical symmetry. Heavier meta particles and lighter ones are randomly distributed in ϕ, θ directions. The value of r is chosen randomly between $(0.25 \times 10^6\ m, 0.75 \times 10^6\ m)$ at the start of the simulation ($t = 0$). This leads to the average radius of the system being fairly similar across all the runs.

C. Stratification based on density

We start with the density of aluminum, $\rho_0 = 8300\,kg/m^3$, across all meta particles, but then 25% of these are made more dense (by 5 times). These densities are then scaled accordingly to make sure that the total mass of the system is approximately the mass of the earth. Note that the densities are not fixed as each particle within a meta-particle still interacts with other particles individually. Here we plot the x, y and x, z positions of the 200 meta particles. The color scheme for the particles is defined by the mass where the more orange means more massive meta particle. We also plot density vs $|r - r_{cm}|$ of each meta-particle where r is the seperation from the center and and r_{cm} is the position of the center of mass of the system for different time t. Here t is the time for which the system has been evolved from $t = 0$. The simulation was ran for $t_{final} = 8\ s$.

We note that we start from a rather disordered arrangement at the first time step $t = 0.1s$, but the system converges to a figure of spherical symmetry as seen from 3. This is seen from the projection on xz and xy plane both resembling a circle (thus indicating spherical symmetry).

We see from our plot in 4, that towards the start, the particles of different densities are evenly distributed. This is inferred from the straight lines that we see at the initial density and the heavier density. The spill overs shown by other particles shows that the system changed from the initial state that was set at $t = 0$. We see after the system has stabilized at $t = 8s$, that there is a clear separation between the two densities. The bigger density

[3] The evaluations can be found in the Mathematica notebook on the attached GitHub link of this project

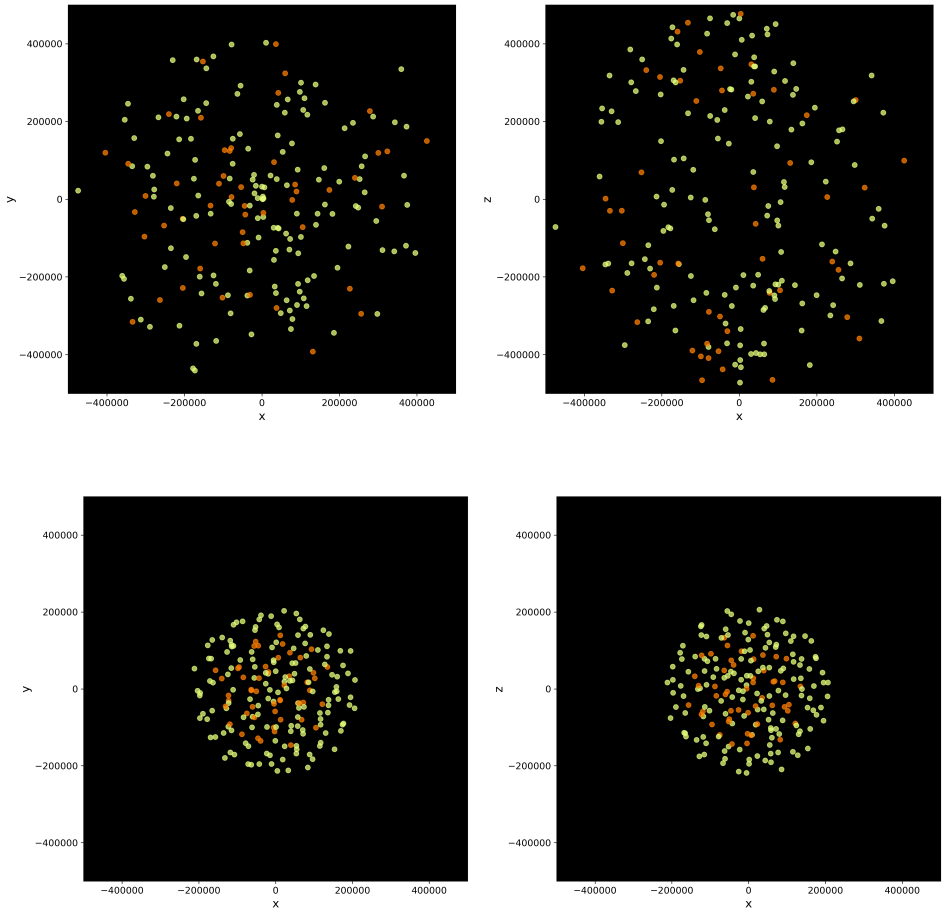

FIG. 3: The x,y and x,z positions of 200 meta-particles at $t = 0.1, 8$ s (top, bottom)

sits closer to the center of mass while the lighter particles are towards the edge (higher separation). This in fact mimics the behavior that we see on earth with a more dense core.

D. Varying other parameters

In this section [4], we do a more systematic study about the various factors affecting the effective radius and velocity of the system, which is approximated by the center of mass positions and velocity in these plots [5].

First we vary K value which is related to pressure by (II.16) while keeping the the three times density fixed at 20%. This means that higher K means a higher P value. This value is changed linearly from 1 to 9 by increments of 2, and for each the plots of r_{cm} vs time (from 0 to 8 s) are plotted. Similarly, we vary ρ values where $\rho_{new} = \rho \times \rho_0$ while keeping $K = 1$ and the percentage of this ρ_{new} at 20%. Lastly, we keep $\rho = 3, K = 1$ fixed while changing the percentage of the more dense material at time $t = 0s$.

[4] The code can be accessed via Github at `https://github.com/Vashistht/Physics_235_Submissions`

[5] Average radius was also plotted which was found to be close to the the center of mass radius and was found to be close to the r_{cm} which shows that the whole system's size is well reflected by r_cm.

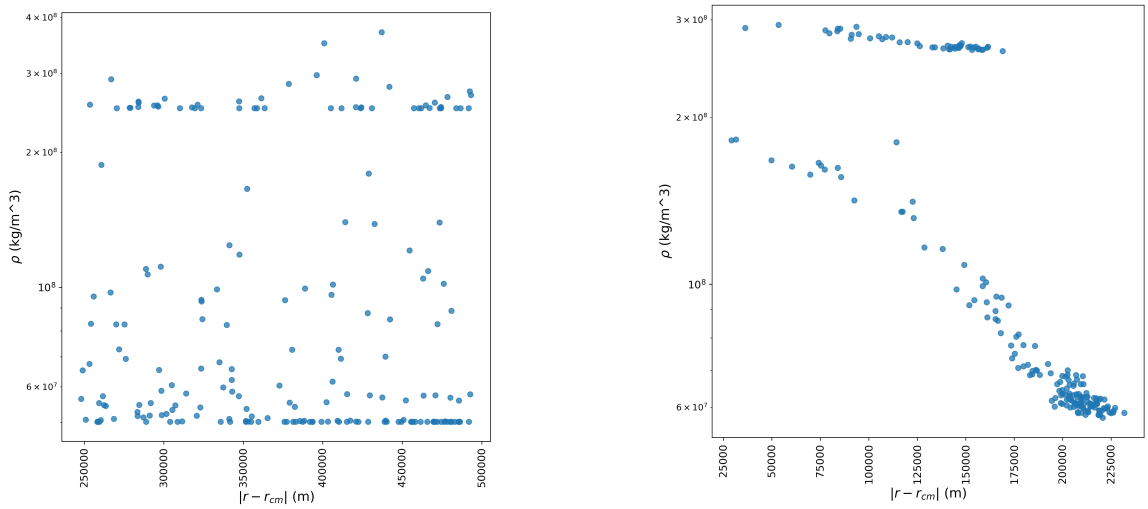

FIG. 4: Plot of density vs the distance of meta-particle from the CM of the system.

We see that the curves in 5 start at a high r_{cm} and v_{cm} and quickly fall off to a certain value. Then they start to show some variation before settling at some value of r_{cm} and v_{cm} (one excepting is the very high density value plot). We note that for 5a, we see the final radius is higher for k value; this is in line with what we expect from the pressure equation. The system reaches a steady state as the effective velocity is 0 after some time t.

For 5b, we change ρ from 1 to $e^4 \approx 54.6$ by multiples of e. e see that the final radius is higher for lower ρ value. This is expected as the denser meta-particles at the start will be found closer to the center. This trend is true for all curves but the one where the density is scaled by 54 times the original. This anomaly also shows a non steady solution. This can be attributed to either the code not accommodating such high difference in ratios or the force of repulsion becoming more prominent. this is in line with what we expect from the pressure equation. The system reaches a steady state where the effective velocity is 0. Note that the effective radius for the highest stable density is lower than what we got by varying K. This can be explained by the fact that pressure depends on ρ^γ as opposed to how K just scales pressure linearly.

Lastly, we vary the percentage of the thrice as dense particles from 2% to 20%. We see that higher the percentage the lower the effective radius. This again lines up with our observation on the stratification and how having more dense material will correspond to reducing the effective radius. The system reaches steady state in this case as well.

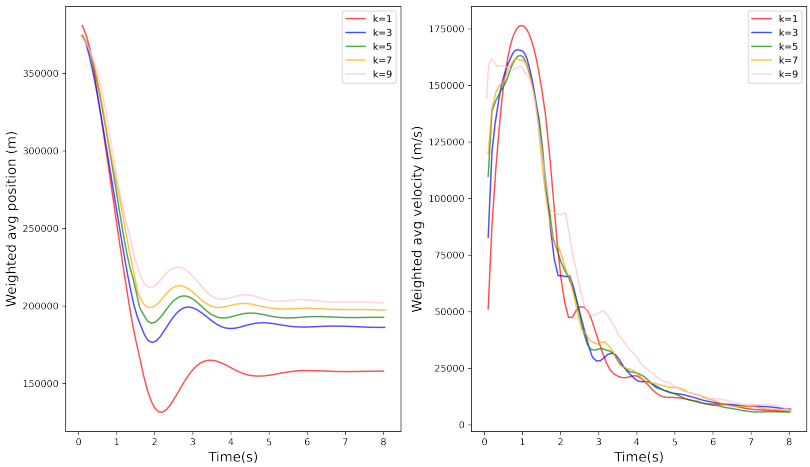

(a) Plotting r_{cm}, v_{cm} vs time for different K values

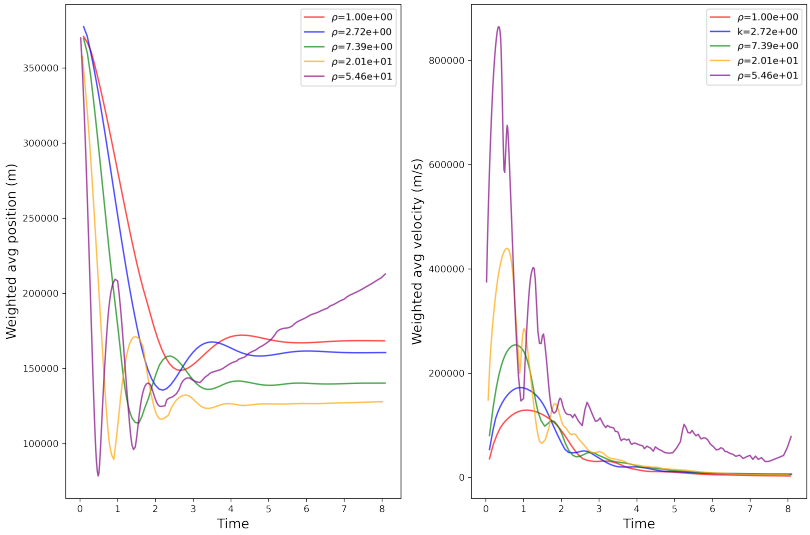

(b) Plotting r_{cm}, v_{cm} vs time for different ρ values

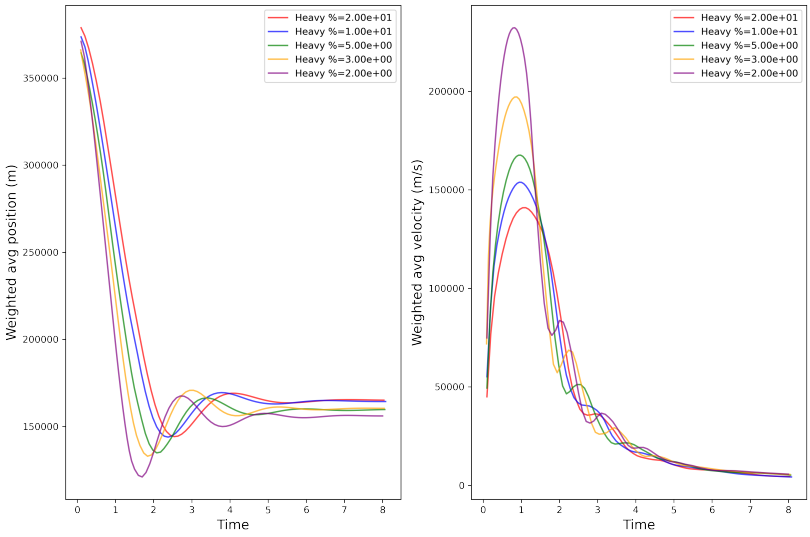

(c) Plotting r_{cm}, v_{cm} vs time by varying % of ρ_{new}

FIG. 5: Varying different parameters and plottingr_{cm}, v_{cm} vs time

IV. DISCUSSION

As we see from the section III, the toy planet gives us a very powerful tool to simulate these systems and see the evolution of these systems. Additionally, this highlights the versatility of SPH method. It is to be noted that the time scale of "planet stabilization" in the toy planet is very short. However, this is not necessarily a problem as the aim is not to predict the time of settlement but to rather see the general trends. However, there are various problems with the analysis and the method used for the analysis itself. In this section, we shed light on both of these shortcomings.

The assumptions were made for the complexity of math involved with more robust settings, and for the ease of simulation. However, these are far from reality. We did not take into account the rise in temperature that happens in these interactions. Additionally, the assumption that pressure was adiabatic and that there was no viscosity again diminish the accuracy of the model in predicting real world behavior. While being able to explain the trends in general, this analysis does not explain more complicated geometries, for example, the layering that we see in planets like Jupiter. Lastly, as seen in the case of time scales of the simulation and planet stabilization, these shortcomings make it hard to calibrate our results with the real world observations.

Apart from the shortcomings of this simple model; there are issues with SPH, the numerical method of choice in the paper. SPH is a very computationally expensive method. Only 10^6 particles were used in the simulation. This was due to the cost of SPH, as it severely limits our ability to scale the system without high-performance computing aid. Additionally, while we did not use boundary conditions in our analysis, SPH is not easy to deal with boundaries where the system changes with the kernel domain Ω.

V. CONCLUSION

In conclusion, the stratification based on density and adiabatic pressure alone (without considering the effects of temperature and other factors) is a rather complicated problem. However, we are able to numerically explain this behavior with the discretization of the flow equations with the aid of Smooth particle hydrodynamics. The theory discussed here is widely applicable to a whole array of problems which makes SPH a great candidate for numerical studies. Like any other model; this one has its own short comings. As discussed in section IV, the toy planet model while being good at explaining trends is far from being predictive. We also saw while SPH offers various improvements over the classical grid based methods by being more versatile, allowing for analytical differentiation, and incorporation for complex geometries, it has its shortcomings. It being very expensive limits our ability to scale this analysis to more massive planets.

In the future, more realistic assumptions like inclusion of viscosity, thermal changes, magnetic interactions, etc. need to be accounted to make the model more robust. One can also explore the effects of different kernel functions on the speed of convergence and the computational cost. Amidst these suggestions, however, we should not forget how with these simplistic assumptions we can explain a rather non trivial problem. This makes for a good

education tool.

[1] G. R. Center, Navier-stokes equations.
[2] P. J. Cossins, Smoothed particle hydrodynamics (2010), arXiv:1007.1245 [astro-ph.IM].
[3] L. B. Lucy, Astronomical Journal **82**, 1013 (1977).
[4] R. A. Gingold and J. J. Monaghan, Monthly notices of the royal astronomical society **181**, 375 (1977).
[5] F. A. Rasio and J. C. Lombardi, Journal of Computational and Applied Mathematics **109**, 213 (1999).
[6] J. J. Monaghan and D. J. Price, Monthly Notices of the Royal Astronomical Society **350**, 1449 (2004), https://academic.oup.com/mnras/article-pdf/350/4/1449/3091165/350-4-1449.pdf.
[7] S. Chandrasekhar, *Newton's Principia for the Common Reader* (Clarendon Press, Oxford, 1995).
[8] S. Manenti, Lecture notes, University of Pavia (2009).
[9] G.-R. Liu and M. B. Liu, *Smoothed particle hydrodynamics: a meshfree particle method* (World scientific, 2003).
[10] M. Kelager, University of Copenhagen: Department of Computer Science **2** (2006).
[11] P. Gourdain and C. Seyler, Plasma summer school (2021).
[12] S. Liu, X. Ban, B. Wang, and X. Wang, Symmetry **10**, 86 (2018).
[13] C. Eckart, The Physics of Fluids **3**, 421 (1960).
[14] V. Springel, Annual Review of Astronomy and Astrophysics **48**, 391 (2010).